GEOLOGICA CARPATHICA, 49, 3, BRATISLAVA, JUNE 1998
181–192

THE CARRIERS OF MAGNETIC PROPERTIES IN THE NEOVOLCANIC ROCKS OF CENTRAL AND SOUTHERN SLOVAKIA (WESTERN CARPATHIANS)

OTO ORLICKÝ

Geophysical Institute, Slovak Academy of Sciences, Dúbravská cesta 9, 842 28 Bratislava, Slovak Republic; geoforky@savba.savba.sk

(Manuscript received March 18, 1997; accepted in revised form March 24, 1998)

Abstract: The carriers of magnetic properties of rocks were studied using: (1) fully automated measurements of magnetic susceptibility (κ) change of sample influenced by temperature in the range of –196 to 700 °C, (2) reflected light microscopy, (3) electron microprobe analysis, (4) Mössbauer spectroscopy, (5) X-ray powder diffraction analysis. The carriers of magnetic properties of the Neogene volcanics have been grouped into seven dominant groups (B, C, D, F, G, I, J) on the basis of the results of method (1) for about 670 individual samples. Groups B–F contain titanomagnetites (TMs) of two magnetic phases of different Curie temperatures (T_{C1}, T_{C2}); Groups B, C: first phase ($T_{C1} \approx$ 130–220 °C) contains quasi homogeneous or partly oxidized TMs of composition $Fe_{2.35}Ti_{0.65}O_4$–$Fe_{2.5}Ti_{0.5}O_4$, second phase ($T_{C2} \approx$ 570–575 °C) contains oxidized TMs of unknown composition. Groups D, F: both magnetic phases correspond to oxidized TMs of unknown composition. Group D — dominant phase of $T_{C1} \approx$ 480 °C and second magnetic phase of $T_{C2} \approx$ 590 °C. Group F contains oxidized TMs, a first magnetic phase of $T_{C1} \approx$ 420 °C and $T_{C1} \approx$ 530 °C, and a second one of $T_{C2} \approx$ 600 °C, $T_{C2} \approx$ 590–600 °C. Magnetic phases of $T_C \leq$ 585 °C also contain small portion of hematite-ilmenites. Group G contains one magnetic phase of $T_C \approx$ 580 °C (and Verwey transition temperature of $T_V \approx$ –153 °C), which corresponds to pure multidomain magnetite. Group I contains two magnetic phases, a first phase of $T_{C1} \approx$ 560–600 °C corresponds to nonstoichiometric magnetite (exceptionally an oxidized TM can be present), and a second phase of $T_{C2} \approx$ 600–630 °C corresponding to hematite-ilmenites. The J group contains only one phase of $T_C \approx$ 610–640 °C. This magnetic phase corresponds to hematite-ilmenites. The magnetic phases of $T_C \approx$ 585–640 °C correspond to hematite-ilmenites, probably of composition within the range $x \approx 0.09$–0.04 (of equation $Fe_{2-x}Ti_xO_3$). Dominant occurrences of the groups B–J have been delineated in the geological schemes.

Key words: Neogene volcanics, 7 dominant groups of Fe-Ti magnetic minerals.

Introduction

In the past a detailed paleomagnetic investigation of neovolcanics of central and southern Slovakia was performed (Orlický 1992; Orlický et al. 1996). Some knowledge about the magnetic minerals of the neovolcanics was also obtained (Nairn 1966; Kropáček et al. 1981; Pašteka 1991; Orlický et al. 1982, 1992; Orlický 1993, 1996). The above presented results concerned only limited collections of rocks.

The results presented in this article were obtained by the study of rock samples collected from about 650 individual localities.

The dominant minerals that are responsible for the magnetic properties in volcanic rocks are within the ternary-system FeO-TiO_2-Fe_2O_3 (McElhinny 1983). In general, diverse chemico-physical conditions (partial pressure, temperature, presence or lack of oxygen, composition of magmatic gases, speed of the ascent and cooling of a magma, presence or lack of magmatic water and steam, etc.) have dominantly influenced the development of magnetic minerals in the volcanic rocks (Kropáček 1986). The crystallization conditions control the composition of the Fe-Ti oxides, while the cooling histories control crystal size, extent of cation-ordering and development transformation microstructures including exsolution and oxidation (Lawson et al. 1987).

In the case of igneous rocks the magnetic minerals (the remanence carriers) are the titanomagnetites (TMs) ($Fe_{3-x}Ti_xO_4$; $0 \leq x \leq 1$; Stacey & Banerjee 1974) or compounds derived by oxidation, substitution and/or unmixing processes (Hargraves & Petersen 1971). The TMs consist of the two end members (spinels) magnetite (Fe_3O_4) and ulvospinel (Fe_2TiO_4). Experience in the study of magnetic minerals have pointed out that they have arisen within the basaltic magma. The basalts and the nepheline-rich rocks contain xenoliths which indicate that these rocks have their source within the mantle (Ehlers & Blatt 1980). In the magnetite-ulvospinel series there is complete solid solution at temperatures in excess of 600 °C. At lower temperatures, the solid solution is much more restricted and there is a tendency for the two phases to exolve (McElhinny 1973). In practice the composition of naturally occurring spinels tends to be displaced towards the hematite-ilmenite series in the direction of increased oxidation. The oxidation during cooling tends to proceed first through the production of ilmenite lamellae and then progresses towards the pseudobrookite series (McElhinny 1973).

Titanohematites are represented by the chemical formula $Fe_{2-x}Ti_xO_3$ where x varies between 0.0 and 1.0. Slow cooling from about 700 °C results in exsolution of hematite-rich ($0 \leq x \leq 0.2$) and ilmenite-rich ($0.8 \leq x \leq 1.0$) components, known as ilmeno-hematites or hematite-ilmenites (Stacey & Banerjee 1974). In the hematite-ilmenite series there is complete solid solution above 1050 °C. At lower temperatures the solid solutions are restricted and the intermediate compositions are represented by the intergrowths of the end members (both rhombohedral) hematite and ilmenite.

Two main alteration processes can determine the state of the Fe-Ti oxides in volcanic rocks: deuteric oxidation, which is active between 800° and 500 °C during initial cooling, and regional hydrothermal alteration, acting between 0° and 300 °C, during post-eruptive burial of younger material (Ade Hall et al. 1971). The true TMs are presumably rare in nature, they are mostly in near-stoichiometric Fe-Ti oxides state. The degree of non-stoichiometry is limited at high temperature (≥400 °C) and the products of such deuteric oxidation beyond the monophasis limit, are intergrowths containing spinel components. The monophasis spinel products of low temperature oxidation are refered to as titanomaghemites and oxidation process itself as maghemitization (O'Donovan & O'Reilly 1976). Kropáček (1986) found that the oxidation process at temperatures up to 400 °C is a diffusive process during which the cation-deficient titanomagnetites (titanomaghemites) are formed, at the temperatures over 500 °C the titanomagnetites undergo spontaneous disintegration and hematite-ilmenites, pseudobrookites and rutiles are formed.

Readman & O'Reilly (1970) studied the alterations of the TMs in detail. They revealed that an original TM was inverted into two-phase intergrowth (spinel and rhombohedral phases) after heating to 700 °C and successive cooling. The spinel phase comprised a mineral close to magnetite (in composition) containing small quantity of Ti and vacancies and a mineral richer in iron than the original TM. The rhombohedral phase comprised a mineral near to ilmenite (less Ti rich in composition than ilmenite), a mineral near to hematite (in composition), pseudobrookite (Fe_2TiO_5) and anatose (TiO_2). The presented knowledge has proved that the Fe-Ti oxides within the rocks are very variable in composition, magnetic state and grain sizes as well as in other characteristics. Though only a very concise description of the Fe-Ti oxides and their possible alterations has been presented above, one can anticipate a high degree of intricacy in the detection and study of natural Fe-Ti minerals in the rocks.

Short outline of geology

Lexa et al. (1993) have distinguished four essential groups of neovolcanic rocks, according to their compositional characteristics and spatial distribution. Only the rocks of two of them have been investigated:

— Areal type andesite volcanic activity including differentiated rocks (this also involves a short episode of acidic rhyolite activity). It lasted since the Early Badenian until the Early Pannonian time. Its spatial distribution was strongly influenced by back-arc extension tectonics associating with diapiric uprising of the mantle. Geochemistry indicates subduction influenced mantle source magmas with variable crustal components.

— Alkali olivine basalt/nepheline basanite volcanic activity in the north-western part of the Pannonian Basin as well as in the southern part of Slovakia. This volcanism was active during the Pannonian to Quaternary periods. Basalts of this type indicate continuing extension accompanied by diapiric uprising in the mantle, which has not been affected by subduction processes.

Shortly about the petrography of the Neogene volcanics:

—Alkaline basalts (according to Mihaliková & Šimová 1989). The alkaline basalts have been divided into the following types: olivine basalts, plagioclase basalts, limburgitic basalts and basanites. The basanites have been divided into the plagioclase basanites, limburgitic basanites, nepheline basanites, amphibole basanites and trachytic basanites. Other dominant types of basalts are the tephrites and trachybasanites. The ore minerals (magnetite, Ti-magnetite, maghemite, ilmenite; in the basanites also ulvospinel and hematite) have been found among the phenocrysts as well as in the matrix of the rocks.

—The products of the areal type andesite volcanic activity (according to Lexa et al. 1997) — the main types of the effusive and extrusive volcanic activity: basaltic andesites, pyroxene andesites, hornblende-pyroxene andesites, pyroxene-hornblende andesites, hornblende andesites, biotite-hornblende andesites to dacites, rhyodacites, plagioclase rhyolites, plagioclase-sanidine rhyolites. The ore minerals (Ti-magnetite, magnetite, ilmenite) have been found among the phenocrysts as well as in the matrix of the rocks. The main types of the intrusive rocks: diorite, granodiorite, aplite, diorite porphyry, basic siliceous-diorite porphyry, acid siliceous diorite porphyry, granodiorite porphyry Zlatno type, granodiorite porphyry Kozí potok type, granite porphyry. The ore minerals (magnetite, Ti-magnetite, ilmenite) have been found among the phenocrysts as well as in the matrix of the rocks.

The contours of individual volcanic formations and complexes are presented in Figs. 1, 2. The individual volcanic formations and complexes including the petrographical characteristics of volcanic rocks are described below Fig. 1.

Experimental techniques

Transmission optical microscopy and reflected light microscopy of the samples were performed by A. Mihalíková and J. Beňka, respectively, in the Geological Survey, Bratislava.

Microprobe analyses, Mössbauer spectroscopy, X-ray diffraction analysis and measurements of magnetic susceptibility (κ) change, as well as electric voltage change of samples influenced by temperature (in low and high temperature intervals) were used to study the magnetic minerals of rocks. The first five methods were performed within the time period 1982–1989. Microprobe analyses were carried out by F. Caňo in the Geological Survey, Bratislava. The compositions of Fe-Ti oxides were studied using the JEOL instrument equipped with the EDAX system. Microprobe analyses were carried out on the compact polished samples (29 samples were observed; 4 or more individual grains of Fe-Ti oxides for each sample were analysed).

The Mössbauer spectroscopy was realized by I. Toth and interpreted by J. Lipka in the laboratory of the Nuclear Physics Dept. of the Slovak Technical University, Bratislava (Lipka et al. 1982–1988). The Mössbauer spectra were recorded using a constant acceleration spectrometer with a source of 1.5 GBq ^{57}Co in rhodium. Isomer shifts have been

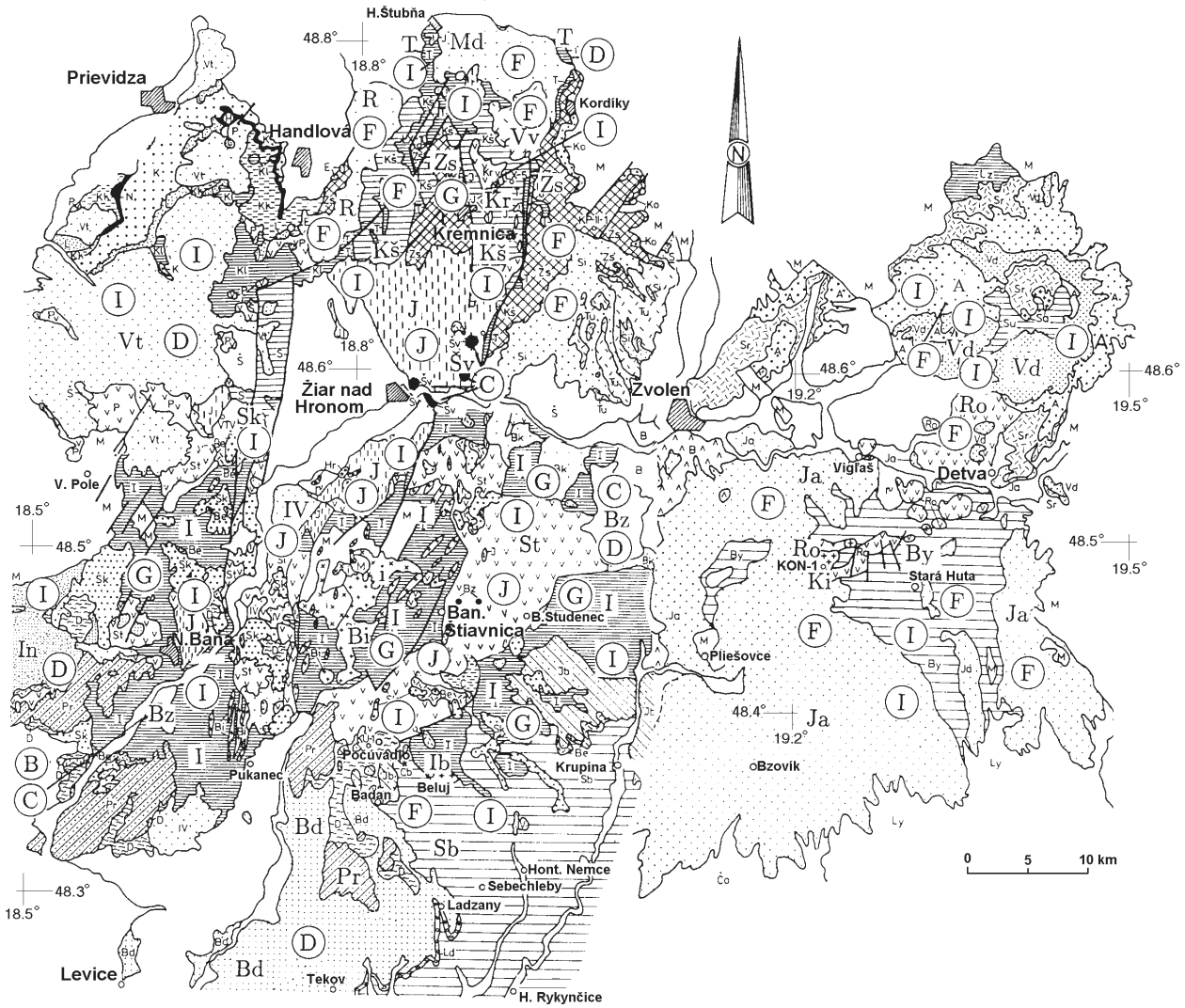

Fig. 1. An outline of the lithostratigraphic units of the volcanics of central Slovakia. (The map has been combined from individual maps, according to V. Konečný et al. 1983). —Products of andesite (and short episode of rhyolite) volcanic activity (2nd group). *Explanations of symbols in the map*: Š — Undivided rocks of the Štiavnica stratovolcano; I — Undivided rocks of the first stage; Zs — Zlatá Studňa Formation (Š, I, ZS — propylitized andesite and andesite porphyry, diorite porphyry, undivided complex of propylitized effusions and intrusions, hornblende-pyroxene, unspecified pyroxene and hypersthene pyroxene andesites). T — Turčok Formation (feldsparic, pyroxene and basaltic andesites); P — Plešina Formation (extrusive domes and subordinate volcanoclastic rocks of hyperstene-hornblende andesites); Si — Sielnica Formation, Vt — Vtáčnik Formation, Jb — Jabloňovývrch Effusive Complex, R — Remata Formation, Md — Flochová Formation, Tu — Turová Formation, Vd — Veľká Detva Formation (Si, Vt, Jb, R, Md, Tu, Vd — pyroxene andesites); Sb — Sebechleby Formation, Sk — Sitno Effusive Complex, Pr — Priesil Formation, A — Abčina Formation, Ja — Javorie Formation, IV — Undivided rocks of the fourth stage (Sb, Sk, Pr, A, Ja, IV — hornblende pyroxene andesites); Bd — Baďan Formation, In — Inovec Formation (Bd, In — glassy pyroxene and feldspharic andesites); St — Studenec Formation, Kr — Krahule Formation (St, Kr — biotite-hornblende andesites); Kš — Kremnický štít Formation (pyroxene-hornblende, pyroxene and biotite-hornblende andesites); Ro — Rohy Formation, B — Neresnica Formation (Ro, B — hornblende-pyroxene, hyperstene-hornblende andesites); Kl — Kľakovská dolina Formation, By — Blýskavica Formation (Kl, By — pyroxene and basaltic andesites); Šv — Šibeničný vrch Complex, Vv — Vlčí vrch Formation (Šv, Vv — basaltic andesites); J — Jastrabá Formation, Hr — Hliník rhyolites (J, Hr — rhyolites and rhyodacites); Ib — Beluj Intrusive Complex, i — Hodruša-Štiavnica Intrusive Complex, Bi — Banisko Intrusive Complex, Ki — Kalinka Intrusive Complex (Ib, i, Bi, Ki — intrusions — andesite porphyry, diorite, diorite-porphyry). Bz — Basalts (the basalts belong to the alkali olivine basalt/nepheline basanite volcanic activity. B, C, D, F, G, I, J (in circuit)— distinguished groups of Fe or Fe-Ti magnetic minerals).

given relative to that of the α-Fe absorber at 27 °C. Ca. 72 samples were analysed. The spectra were obtained at absorber laboratory temperature, but seven samples of magnetic fraction from basalts were also measured at liquid nitrogen temperature where the hopping among the octahedral Fe^{2+} and Fe^{3+} ions in the Fe-Ti oxides does not occur.

X-ray powder diffraction analyses were performed by B. Toman in the Geological Institute of the Slovak Academy of

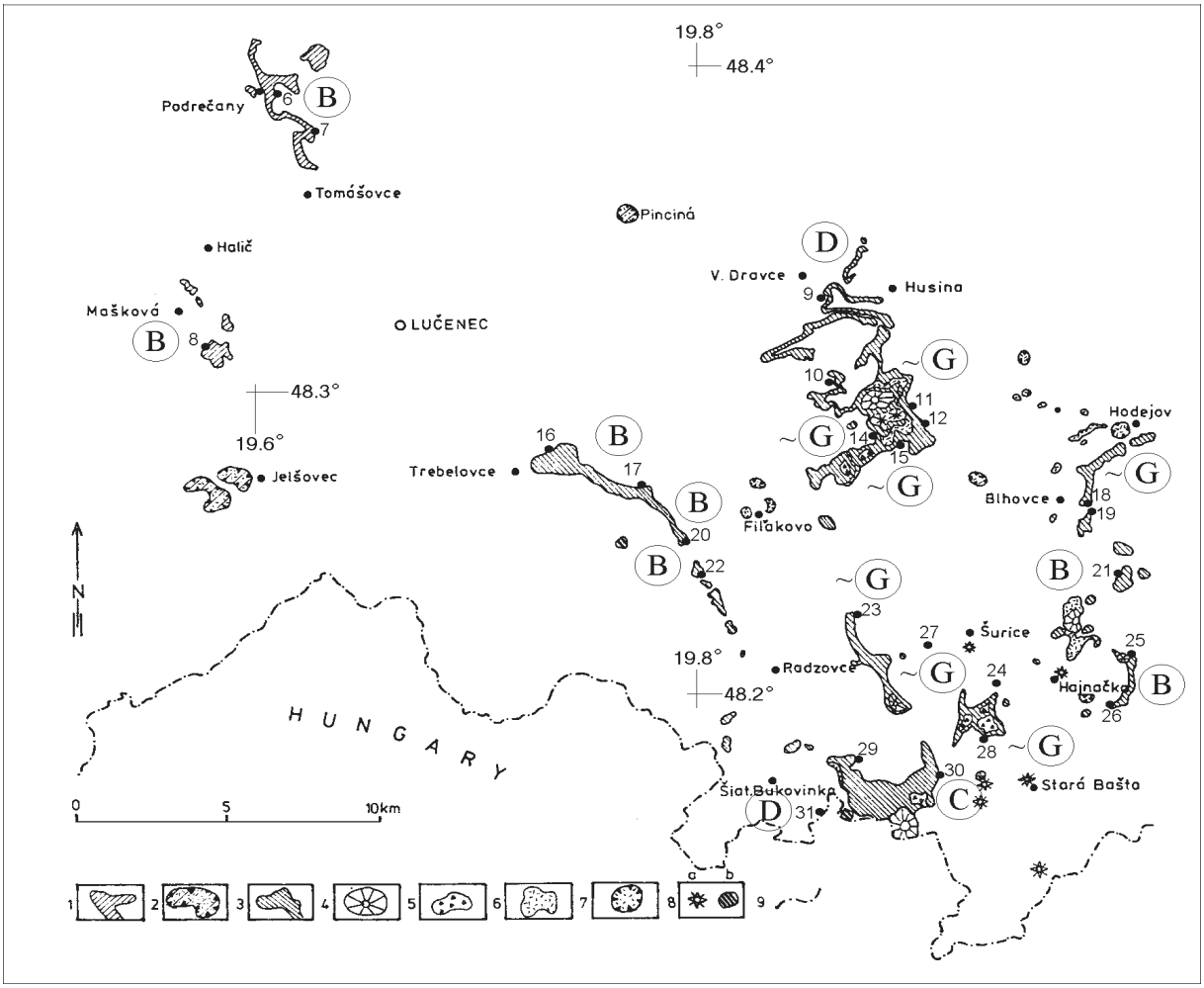

Fig. 2. Scheme of relicts of alkali basalt volcanism of southern Slovakia (according to Vass & Elečko 1992). 1 — lava flows of Podrečany Basalt Formation; 2 — maars of the Podrečany Basalt Formation; 3 — lava flows of the Cerová Basalt Formation; 4 — cinders cones; 5 — agglomerates; 6 — lapilli tuffs; 7 — maars of the Cerová Basalt Formation; 8 — feeding systems of the Cerová Basalt Formation: a) diatremes, b) necks; 9 — frontiers between Slovakia and Hungary. 6–31 near of dots-numbers of localities. B, C, D and ~G (in circuit) — selected groups of Fe-Ti magnetic minerals.

Sciences, Bratislava. The Philips PW 1420 X-ray spectrometer and PW 1150 diffractometer were used to perform the powder diffraction analyses of samples. Co-Kα, Cu radiation using the Fe filter was applied. A total of 52 samples were analysed.

Measurements of the change of electric voltage of samples of the magnetic fraction influenced by temperature (from liquid helium temperature to room temperature) were performed by A. Zentko in the Institute of Experimental Physics of the Slovak Academy of Sciences, Košice.

Measurements of magnetic susceptibility (κ) change in samples influenced by temperature were performed by the author of this article. The description of the apparatus and laboratory procedure have been published by Orlický (1990). This method is fully automated. It is able to detect all subtle magnetic phases and their tendency to change due to the influence of temperature (in the presence or absence of oxygen) on the rocks. The measurements by this method were performed with the presence of air oxygen (except the sample presented in Fig. 4). The samples from about 650 outcrops were studied by this method. The powdered samples were prepared by grinding, subsequent magnetic separation, (mostly by bar permanent magnet; but several samples were separated by Cook, or Kaldrovich magnetic separators). Some samples were separated by the flotation method by M. Žabka at the Geological Institute of the Slovak Academy of Sciences, Bratislava. We also tried to separate individual magnetic components from each other, but this procedure was almost ineffective due to the mutual intergrowth of magnetic grains within the rocks.

Results and the contribution of individual methods

The results of the transmission optical microscopy have been mainly used for the more precise petrographical description of the rocks.

The results obtained by all methods have been presented in Tables 1, 2, 3. We see from Tables1–3 that 3 types of magnetic oxides were detected in the rocks using the re-

Table 1: The results of reflected light microscopy, Curie temperature measurements, X-ray diffraction analyses, electron microprobe analyses and Mössbauer spectroscopy of magnetic minerals.

Group	Number of samples	Type of rock	Geographical coordinates		Reflected light microscopy	Curie temperature of magnetic phases	Mössbauer spectroscopy	X-ray diffraction analyses	Microprobe analyses		
			φL(°)	ϑL(°)					Grain size (μm)	FeO (%)	TiO_2 (%)
B	148a/7	Basaltic andesite	48.451	18.81		$T_{C1} \approx 130$ °C $T_{C2} \approx 570$ °C		TM	25 15 10 7	72.49 73.35 73.41 72.99	25.78 25.07 24.58 25.53
B	Brehy B2/16	Nepheline basanite	48.409	18.650		$T_{C1} \approx 220$ °C $T_{C2} \approx 570$ °C		TM Pbr	20 10 8 7 6	76.64 74.36 75.84 74.26 73.48	22.42 23.77 23.20 24.57 25.63
C	Š.V.6/1	Aphanitic basaltic andesite	48.593	18.879		$T_{C1} \approx 210$ °C $T_{C2} \approx 575$ °C		TM Mag Hem Ilm	20 10 8 7	71.73 75.97 71.86 75.61	26.16 23.25 25.84 23.08
	Š.V.3/2	„	48.593	18.879		$T_{C1} \approx 210$ °C $T_{C2} \approx 575$ °C			60 8 8 8 7	73.23 74.44 74.44 73.49 75.61	24.63 23.83 23.83 24.58 23.08
D	Bd-256/2	Glassy pyroxene feldsparic andesite	48.280	18.750		$T_{C1} \approx 480$ °C $T_{C2} \approx 590$ °C					
	Vt-45/11	Pyroxene andesite	48.550	18.600		$T_{C1} \approx 480$ °C $Tc_2 \approx 590$ °C	TM(35%) Mag(40%) Magh(6%)		100 50 10 6	78.90 78.26 82.75 82.33	17.34 18.56 14.51 13.69
F	Kr. Vr.-26/1	Hyperstene augite andesite	48.757	18.817		$T_{C1} \approx 420$ °C $T_{C2} \approx 600$ °C					
	AF-329-B2	Pyroxene hornblende andesite	48.653	19.344		$T_{C1} \approx 530$ °C $T_{C2} \approx 590$ °C– –600 % °C	Mag(57%) Hem(6%) Magh(10%)	Mag Magh Rutile	30 15 6	83.32 80.35 84.94	15.43 18.88 14.68
G	I-104/1	Propylitized pyroxene andesite	48.483	18.750		$T_C \approx 580$ °C $Tv \approx -153$ °C	Mag(100%)	Mag Rutile	100 70 50 15	93.16 94.86 94.05 0.82	4.43 3.86 3.25 99.18
	I-181/4	„	48.439	18.849		$T_C \approx 580$ °C $Tv \approx -153$ °C					
I	St-156/1	Biotite-hornblende andesite	48.451	18.966		$T_{C1} \approx 580$ °C $T_{C2} \approx 620$-630 °C	Mag(13%) Hem(48%) Magh(27%)	Mag Hem	100 40 12 7	79.03 89.35 97.67 98.35	20.60 8.65 0.29 0.68
	St-215/4	„	48.412	18.723		$T_{C1} \approx 580$ °C $T_{C2} \approx 620$–630 °C $Tv \approx -153$ °C					
J	3-IV-B1/1	Hornoblende-pyroxene andesite	48.518	18.743		$T_C \approx 630$ °C	Mag(30%) Hem(30%) Ilm	Mag Magh Hem	60 70 10 10 10 7 7 6 6	76.60 89.24 93.91 56.19 88.72 91.30 95.08 53.64 78.81	23.40 9.52 5.04 43.81 11.28 8.70 0.00 45.40 20.41
J	TR-24	Hyperstene -hornblende -biotite andesite	48.456	18.947	Hem Mag	$T_C \approx 640$ °C	Mag(16%) Hem(22%) Magh(14%) Ilm	Magh Hem	45 30 20 7	84.40 55.10 93.38 90.20	14.53 44.12 5.34 8.40

Mag—magnetite; Hem—hematite; Magh—maghemite; Ilm—ilmenite; Us—ulvospinel; Br—brookite; Pbr—pseudobrookite; TM—titanomagnetite.

flected light microscopy. Magnetite (Mag) was detected in all samples, hematite (Hem) was detected in 14 samples and ilmenite (Ilm) was detected in 5 samples of rock. These minerals mostly intergrow each other when they are present together in the rock.

Electron microprobe analysis

Electron microprobe analysis can detect only the chemistry of the respective material. The contents of FeO and TiO_2 of samples were presented in Tables 1–3. The compositional

Table 2: The results of reflected light microscopy, Curie temperature measurements, X-ray diffraction analyses, electron microprobe analyses and Mössbauer spectroscopy of magnetic minerals.

Group	Number of samples	Type of rock	Geographical coordinates		Reflected light microscopy	Curie temperature of magnetic phases	Mössbauer spectroscopy	X-ray diffraction analyses	Microprobe analyses		
			ϕ L (°)	λL (°)					Grain size (μm)	FeO (%)	TiO_2 (%)
I	St-4/1	Pyroxene andesite	48.610	18.583		$T_{C1} \approx 600$ °C $T_{C2} \approx 620$ °C	Mag (30%) Hem (21%) Magh (25%) TM (11%) Ilm	Mag, Hem	40 20 10 5	50.72 50.74 88.27 90.36	49.02 48.65 11.05 9.11
D	Vt-16/2	Pyroxene andesite	48.613	18.611		$T_{C1} \approx 500$ °C $T_{C2} \approx 590$ °C	Mag (20%) TM (59%) Ilm	Mag, Magh, Ilm			
J	Vt-38/3	Autometa-morphosed pyroxene andesite	48.567	18.714	Mag Hem	$T_C \approx 610$ °C		Mag, Hem, Magh	70 70 30 7	93.73 60.54 93.60 92.39	5.27 38.94 6.00 6.37
J	St-43/3	Pyroxene andesite	48.566	18.500		$T_C \approx 615$ °C	Mag (36%) Magh (21%) Hem (25%) Ilm	Mag, Hem, Ilm Us, Pbr Br			
I	TR-13/2	Hornblende pyroxene andesite	48.548	18.670	Mag Hem	$T_{C1} \approx 580$ °C $T_{C2} \approx 620$ °C	Mag (26%) Hem (33%) Magh (8%) TM (11%)	Mag, Hem Magh	60 8 7 7	91.18 73.93 96.49 88.40	8.14 25.56 3.27 11.12
I	Tr-16/1	Hyperstene -hornblende biotite andesite	48.509	18.656	Mag Hem TM	$T_{C1} \approx 600$ °C $T_{C2} \approx 615$ °C	Mag (44%) Hem (21%) Magh (11%) Ilm	Mag, Hem, Magh Ilm Br	40 30 15 10	92.31 50.90 87.41 87.41	7.48 48.64 12.34 12.34
I	TR-16/3	Hyperstene hornblende-biotite andesite	48.509	18.656	Mag Hem Ilm	$T_{C1} \approx 600$ °C $T_{C2} \approx 620$ °C	Mag (37%) Hem (35%) Ilm	2 samples: Hem 1 sample: Magh, Br 2 samples: Mag, Hem 2 samples: Mag, Hem, Br 7 samples: Mag, Hem, Ilm, Br	60 60 15 15 6 5	91.98 65.79 91.73 70.09 90.14 88.28	7.50 33.83 7.67 29.42 8.85 10.90
J	St-102/13	Biotite-hornblende andesite	48.482	18.745		$T_C \approx 630$ °C	Mag (%) Hem (55%) Magh (29%) Ilm	Magh, Hem Us, Ilm Br	40 20 10 7	92.65 88.20 81.83 80.21	7.02 11.51 17.88 19.01
I	I-238/7	Pyroxene andesite	48.382	18.633		$T_{C1} \approx 590$ °C $T_{C2} \approx 620$ °C	Mag (82%) Hem (3%) TM (10%)	Mag, Hem	30 20 10 7	78.05 51.02 77.56 76.29	18.89 48.39 19.09 20.97
G	TR-6/2	Hyperstene hornblende biotite andesite	48.578	19.345	Mag Hem	$T_C \approx 580$ °C	Mag (82%) Hem (8%)	Mag, Hem Br	30 15 15 10 10	85.13 91.00 53.99 54.23 52.11	13.96 8.62 45.86 45.57 47.42
F I	TR-11	Hornblende pyroxene andesite	48.550	19.331	2 samples Mag Hem TM 3 samples Hem Ilm	$T_{C1} \approx 530$ °C $T_{C2} \approx 590$ °C $T_{C1} \approx 560$ °C $T_{C1} \approx 615$ °C	2 samples: Mag (70%) Hem (10, 15%) Ilm 2 samples: Mag (51, 67%) Hem (22, 17%) Magh (17, 8%) Ilm 1 sample: Mag (42%) TM (36%) Ilm Nonmagn. fr.: 2 samples: Mag (12, 18%) Hem (28, 30%) Ilm 1 sample: Hem (42%), Ilm	1 sample: Mag, Hem, Magh 2 samples: Hem, Ilm 1 sample: Hem, Ilm, Magh 4 samples: Mag, Hem, Ilm 2 samples: Mag, Hem, Ilm, Us 2 samples: Mag, Hem Us, Pbr 1 sample: Mag, Hem, Magh, Pbr 1 sample: Mag, Hem, Magh, Ilm, Us, Pbr	70 10 7 7 6 70 60 10 7 7 70 60 8 7 7 80 30	80.77 99.05 82.11 88.47 91.89 95.72 52.57 83.97 93.51 97.47 95.13 47.83 68.68 91.07 68.53 46.70 90.36	18.91 0.12 17.47 11.39 8.11 4.02 46.17 15.41 5.79 1.15 4.51 51.45 30.98 8.93 30.84 52.22 9.40

Mag—magnetite; Hem—hematite; Magh—maghemite; Ilm—ilmenite; Us—ulvospinel; Br—brookite; Pbr—pseudobrookite; TM—titanomagnetite.

Table 3: The results of reflected light microscopy, Curie temperature measurements, X-ray diffraction analyses, electron microprobe analyses and Mössbauer spectroscopy of magnetic minerals.

Group	Number of samples	Type of rock	Geographical coordinates		Reflected light microscopy	Curie temperature of magnetic phases	Mössbauer spectroscopy	X-ray diffraction analyses	Microprobe analyses		
			ϕ L (°)	λL (°)					Grain size (μm)	FeO (%)	TiO_2 (%)
J	TR-15/1	Hornblende -pyroxene andesite	48.544	18.947	Mag Hem	$T_C \approx 610\ ^\circ C$	Mag (52%) Hem (12%) Magh (9%) TM (8%), Ilm	Mag, Hem Ilm,TM			
F	TR-17/2	Biotite hornblende andesite	48.509	18.973	Mag	$T_{C1} \approx 520\ ^\circ C$ $T_{C2} \approx 570\ ^\circ C$	Mag (49%) TM (51%)	Mag, Hem	40 20 10 7	88.65 87.95 83.70 88.30	10.31 10.17 14.76 10.00
J	TR-19/1	Pyroxene andesite	48.461	18.971	Mag	$T_C \approx 610\ ^\circ C$	Mag (74%) TM (4%) Ilm	Mag			
J	TR-20/2	Hornblende biotite andesite	48.462	18.971	Mag Hem	$T_C \approx 612\ ^\circ C$	Mag (30%) Hem (35%) Magh (12%), Ilm	Hem, Ilm Magh, Br			
I	TR-22/1	Hornblende -biotite andesite	48.457	18.941	Mag	$T_{C1} \approx 570\ ^\circ C$ $T_{C2} \approx 620\ ^\circ C$	Mag (47%) Hem (22%) Magh (9%), Ilm	Mag, Hem Ilm, Br			
J	TR-23/2	Hornblende -biotite andesite	48.427	18.898	Mag Hem Ilm	$T_C \approx 625\ ^\circ C$	Mag (53%) Hem (24%)	Mag	15 8 6	82.27 90.13 87.69	15.64 8.60 10.37
J	Tr-25/2	Biotite -hornblende andesite	48.450	18.965	Mag	$T_{C1} \approx 625\ ^\circ C$	Mag (55%) Hem (23%) Magh (8%), Ilm	Mag, Hem, Br			
J	I-174/3	Pyroxene andesite (propylized)	48.445	18.883		$T_C \approx 620\ ^\circ C$		Mag	40 15 10 7	0.41 3.15 1.38 2.19	99.59 96.05 98.62 96.98
I	AF-314A1	Pyroxene andesite	48.665	19.392		$T_{C1} \approx 580\ ^\circ C$ $T_{C2} \approx 600\ ^\circ C$	Mag (78%) Hem (12%) Ilm	Mag, Hem Ilm			
J	AF-323/1	Augite -hyperstene andesite	48.660	19.400		$T_C \approx 630\ ^\circ C$	Mag (16%) Hem (20%) Ilm	Hem, Magh	100 30 10 6	63.87 50.47 94.19 60.93	34.79 49.00 3.64 38.38
I	VD-331B1	Pyroxene -biotite andesite	48.650	19.392		$T_{C1} \approx 565\ ^\circ C$ $T_{C2} \approx 605\ ^\circ C$	Mag (59%) Hem (28%) Magh		50 15 10 6	87.50 86.17 88.35 87.04	11.71 13.42 10.73 12.73
I	VD-335A3	Pyroxene -biotite andesite	48.647	19.380		$T_{C1} \approx 575\ ^\circ C$ $T_{C2} \approx 605\ ^\circ C$	Mag (43%) Hem (33%) Magh (12%) Ilm	Mag, Hem	40 40 15 7	51.87 91.69 93.01 92.43	47.70 8.31 6.99 7.57
I	Ro-399	Pyroxene -hornblende hyperstene andesite	48.583	19.373		$T_{C1} \approx 570\ ^\circ C$ $T_{C2} \approx 620\ ^\circ C$	Mag (37%) Hem (51%) Magh (5%) Ilm	Mag, Hem Magh	90 30 15 6	86.97 46.17 46.96 54.95	11.50 52.31 51.12 44.24
F	Ro-404B1	Pyroxene -hornblende andesite	48.575	19.397		$T_{C1} \approx 520\ ^\circ C$ $T_{C2} \approx 610\ ^\circ C$		Mag, Hem			
F	Ro-405C1	Pyroxene -hornblende andesite	48.573	19.387		$T_{C1} \approx 530\ ^\circ C$ $T_{C2} \approx 590\ ^\circ C$	Mag (92%) Ilm	Mag, Hem Ilm			
F	Ro-427A1	Pyroxene -hornblende andesite	48.550	19.390		$T_{C1} \approx 520\ ^\circ C$ $T_{C2} \approx 590\ ^\circ C$	Mag (69%) TM (23%)	Mag, Magh			
I	Ja-450	Pyroxene -hornblende andesite	48.485	19.400		$T_{C1} \approx 590\ ^\circ C$ $T_{C2} \approx 610\ ^\circ C$	Mag (87%) Hem (8%)	Mag, Hem Ilm			
F	Ja-451D1	Pyroxene -hornblende andesite	48.477	19.347		$T_{C1} \approx 520\ ^\circ C$ $T_{C2} \approx 600\ ^\circ C$	Mag (67%) TM (14%) Magh (6%)	Mag, Magh			

Mag—magnetite; Hem—hematite; Magh—maghemite; Ilm—ilmenite; Us—ulvospinel; Br—brookite; Pbr—pseudobrookite; TM—titanomagnetite.

parameter x for TM was calculated using the Ti/Fe ratio according to Furuta (1993). The first magnetic phase of basalts and basaltic andesites (Table1) contains quasi homogeneous or partly oxidized TMs of a composition $Fe_{2.35}Ti_{0.65}O_4$–$Fe_{2.5}Ti_{0.5}O_4$. Several samples of andesitic rocks have pointed out also rather homogeneous contents of FeO or TiO_2 in most of individual grains (see Tables1–3), but the Ti/Fe ratio of individual grains is significantly lower compared with that for basalts and basaltic andesites. Oxidized-cation deficient TMs are present in these rocks. The general formula for oxidized TM is $Fe^{3+}_{8/3-2x}Fe^{2+}_{x}Ti^{4+}_{x}\square_{1/3}O^{2-}_{4}$, when oxidation is complete (□ denotes the lattice vacancies, Stacey & Banerjee 1974). Because the oxidation parameter "z" (or a degree of oxidation) of the TMs has not been determined the compositional parameter x for cation deficient TMs has not been derived. The samples of rock I-104/1 (Table 1) or I-174/3 (Table 3) do reflect quite uniform dominant contents of FeO (I-104/1), or uniform dominant volumes of TiO_2 (I-174/3), among individual grains. A dominant portion of Mag and minor portion of rutile is present in sample I-104/1, and a dominant portion of rutile and minor portion of other Fe-Ti oxides is present in sample I-174/3. In samples of rocks of variable-heterogeneous contents of FeO and TiO_2 quantities (Tables 1–3), a presence of ilmenite (Ilm) in respective grain has been predicted on the basis of FeO and TiO_2 contents, compared with the data (FeO = 46.54 %, TiO_2 = 45.70 %), published by Lawson & Gordon (1987) for the ilmenite from the Ilmen Mountains, USSR.

Mössbauer spectroscopy

In principle, Mössbauer absorption spectra of magnetic spinels and their paramagnetic and ferrimagnetic states should provide useful information about the valence state of the cations, their distribution between octahedral and tetrahedral sites, and deviations from perfect cubic symmetry. In practice, however, only the "normal" spinel data, where each site contains only one kind of cation can be interpreted with a high degree of confidence. In inverse spinels complications can arise in interpretation of the results (Banerjee et al. 1967). Basically linewith, isomer shift (IS), quadrupole splitting (QS) and hyperfine field of the spectrum are characteristics for respective Fe or Fe-Ti minerals. Unfortunately, in Fe-Ti oxides we can find some difficulties in these parameters. For example ilmenite ($FeTiO_3$) and pseudobrookite (Fe_2TiO_5) have rather the same range of QS and IS. Room temperature spectra with increasing portions of Ti^{4+} ions in TM also in titano-hematites become progressively more difficult to analyze because of broadening and overlapping of the peaks of the spectrum (Warner et al. 1972). Such a result is not interpretable according to standard procedures. Fe-Ti oxides of basaltic rocks (Table 1) were measured at room temperature as well as at the liquid nitrogen temperature. While the spectra at room temperature were broad (non Lorentzian lines), on cooling to –196 °C, one set of six lines was sharpened dramatically. The parameters of the spectra correspond rather to magnetite, but with relatively broad lines. Similar results have been published by Banerjee et al. (1967). According to their suggestion the results suggest that at –196 °C there is no hopping of the electrons among the octahedral Fe^{2+} and Fe^{3+} ions, so that the observed spectrum is the sum of that from Fe^{2+}, which is broad and similar to that of Fe_2TiO_4, and Fe^{3+}, which is an almost spherically symmetrical ion and gives sharp lines as it is not so sensitive to the random environment. We know that individual magnetic minerals are present in different grain size in the sample. The Mössbauer spectroscopy is very sensitive to the grain size of the studied sample. For example while Hem of about 18 nm has a typical sextet's spectrum, Hem of about 5 nm appears as a typical doublet's, paramagnetic spectrum.

Most of the Mössbauer's spectra of the Fe-Ti oxides from the andesitic rocks were interpreted despite the above described difficulties. The interpretation of Ilm is considered problematic. Its presence has been only predicted in respective rocks. Most andesitic rock samples contain Mag, Hem, Magh, in some samples also TM or Ilm, according to Tables 1–3. Their relation is very different.

X-ray powder diffraction analysis

We can use the results of analyses to make only a rough image about the composition of the Fe-Ti oxides. We know that the unit cell size increases with the amount of the Fe_2TiO_4 within the titanomagnetite (from 8.39 Å for pure Fe_3O_4 to 8.53 Å for pure Fe_2TiO_4, McElhinny 1973). Similarly the unit cell parameter (a_{rh}) increases with the amount of ilmenite ($FeTiO_3$) within the hematite-ilmenite (from 5.42 Å for pure α-Fe_2O_3 to 5.54 Å for pure ilmenite, McElhinny 1973). This means that the composition of the Fe-Ti oxide might have been determined very effectively on the basis of the unit cell parameters. Due to intricate interferences, the X-ray diagrams were not suitable for deriving the unit cell sizes of the Fe-Ti oxides. Only a qualitative interpretation of the X-ray diagrams were made. (We derived the lattice constants of some samples of the TMs using the equation of Hamano (1989), for basalts for the temperature 20 °C in the past, Orlický et al. (1992); they are: d = 8.455–8.489 Å, for x = 0.3–0.73).

Measurements of the magnetic susceptibility change of samples influenced by temperature

The method can use the following effects for the detection of different magnetic phases within the magnetic material:

— The Curie temperature (T_C) which is a characteristic constant for both, ferromagnetic or ferrimagnetic materials. The Curie temperatures of TMs are dependent primarily on the concentration of cations found on the octahedral and tetrahedral lattice sites and are dependent in only a subordinate way on the cation distribution (O'Reilly 1984).

— The Verwey transition temperature (T_V) of magnetite at about –155 °C (magnetite undergoes a cubic-to-orthorombic crystallographic transition on cooling through –155 °C, Stacey & Banerjee 1974). This effect is accompanied by the

presence of magnetic susceptibility (κ, or other magnetic parameter's) peak at about –155 °C; it is the so-called isotropic point. However, the isotropic point itself is very sensitive to departures from stoichiometry of the magnetite and generally will be lowered for impure samples (Syono & Ishikawa 1963). The presence of a well defined isotropic peak in magnetite constitutes a diagnostic feature of the multidomain state (Radhakrishnamurty et al. 1981).

— A decreasing of the κ of the titanomagnetites from room temperature down to liquid nitrogen temperature. This effect was studied by Senanayake & McElhinny (1982) on the magnetic fraction of basaltic rocks, and by Radhakrishnamurty & Likhite (1993) on synthesized titanomagnetites.

— A decreasing of the κ of maghemitized magnetite over 280 °C due to transformation of maghemitized part of magnetite (if any) into hematite influenced by temperature. This effect appears more conspicuous with decreasing of the grain size of magnetic particles.

— The Morin transition of hematite. In hematite, the spin moments above –10 °C are oriented in the c plane, but instead of being precisely antiparallel, they are slightly canted, resulting in a weak spontaneous magnetization within the c plane, but normal to the spin-axis. Below –10 °C, due to change in the sign of the magnetocrystalline anisotropy, the c-axis becomes the spin axis (Stacey & Banerjee 1974). This effect is accompanied by a sharp decreasing of the κ, or other magnetic parameter of hematite, being cooled e.g. from room temperature to below –10 °C. This effect depends very strongly on the stoichiometry of hematite, in some non-stoichiometric hematites it is completely missing.

— The Néel temperature (T_N) for the detection of the stoichiometric ilmenite at about –218 °C. In the hematite-ilmenites the Néel temperature ranges in the –218 °C (ilmenite) to 675 °C (for hematite) temperature interval, depending on the content of ilmenite in hematite (Nord & Lawson 1989; McElhinny 1973). Several samples of hornblende pyroxene andesite of locality 3-IV-B1 (group J) were studied by the method of electric voltage change of a sample influenced by temperature, in the interval from laboratory temperature down to liquid helium temperature.

The presence of non-stoichiometric ilmenite was detected by this method.

Moreover, if the Curie temperatures of synthetic TMs of defined composition are known, the compositional parameter (x) of a respective sample of natural Fe-Ti oxide can be derived (e.g. magnetic phases of samples 148a/7 and B2/16, with the range $T_C \approx 130$–220 °C, Table 1, correspond to the composition of $Fe_{2.3}Ti_{0.7}O_4$–$Fe_{2.4}Ti_{0.6}O_4$, and magnetic phases of samples Kr.Vr.-26/1 and Bd-256/2 with the range $T_C \approx 420$–480 °C, Table 1, correspond to the compostion of $Fe_{2.7}Ti_{0.3}O_4$–$Fe_{2.8}Ti_{0.2}O_4$, comparing our results with those published by Radhakrishnamurty et al. (1981) for synthetic TMs of defined parameter x). The composition of Ti^{4+} in TM derived by this procedure is supposed to be rather higher compared with that derived from the Ti/Fe ratio according to Furuta (1993). (The data presented by Radhakrishnamurty et al. 1981 were obtained on synthetic, stoichiometric T_M, whereas the data presented by Furuta (1993), were derived from the results of natural Fe-Ti oxides; other discrepancy can result from a different oxidation of TM; e.g. a TM of x = 0.6 could have $T_C \approx 175$ °C for oxidation parameter z = 0.0, but $T_C \approx 490$ °C for z = 1.0, according to Néel–Chevallier theoretical calculation; in Moskowitz 1987).

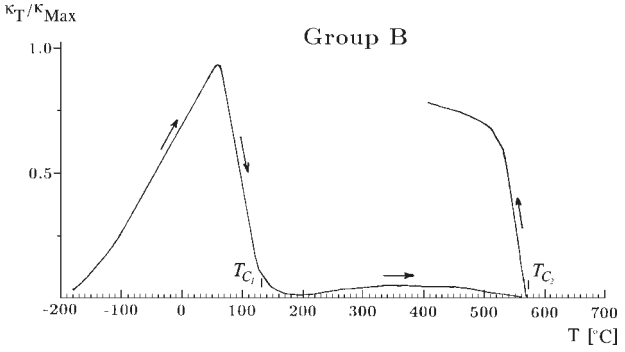

Fig. 3. Thermomagnetic curve of sample No. 148a/7 (basaltic andesite). The sample contains two magnetic phases — $T_{C1} \approx 130$ °C; $T_{C2} \approx 570$ °C; κ_T — magnetic susceptibility of the sample at temperature T, κ_{Max} — maximum magnetic susceptibility of the sample among all the data within the whole applied temperature interval. T_C — Curie temperature of concrete magnetic phase. T — temperature. → heating of sample, ← cooling of sample. The explanations of T, κ_{Max},T_C,T, →, ←, are also valid for Figs. 4–10.

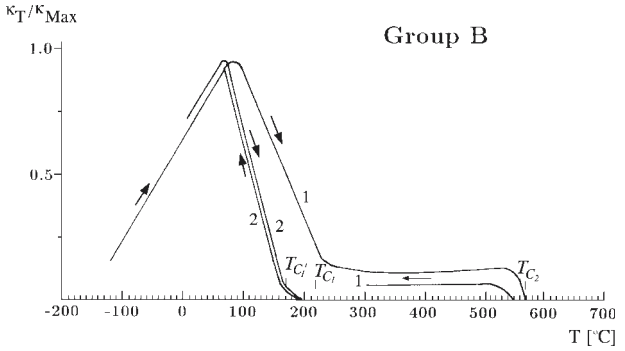

Fig. 4. Thermomagnetic curves of sample No. B2/16 (nepheline basanite). Sample contains two magnetic phases —$T_{C1} \approx 220$ °C; $T_{C2} \approx 570$ °C. Curve 1 — measurements of the sample in air; Curve 2 — measurements in a vaccuum ($\approx 10^{-5}$ Torr). Only one phase with $T_{C1} \approx 170$ °C has been detected after heating of the sample to 700 °C and successive cooling in a vacuum.

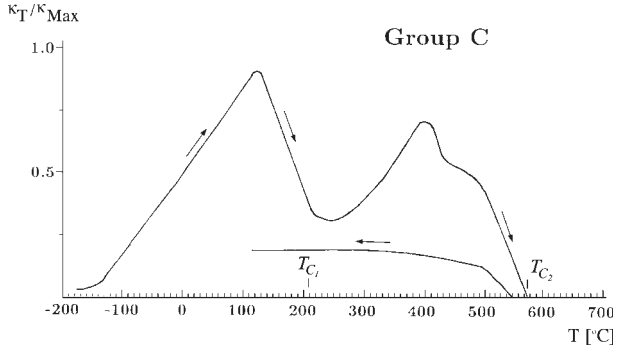

Fig. 5. Thermomagnetic curves of sample No. ŠV-6/1 (aphanitic basaltic andesite). The sample contains two magnetic phases $T_{C1} \approx 210$ °C; $T_{C2} \approx 575$ °C.

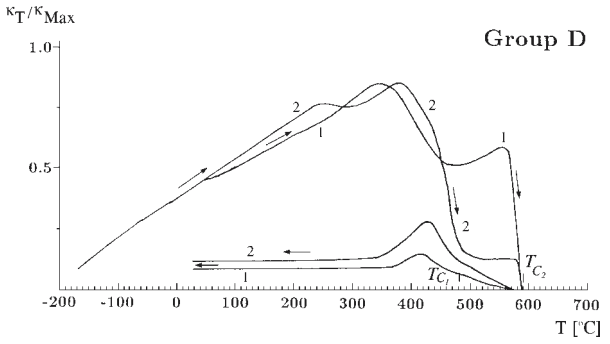

Fig. 6. Thermomagnetic curves of samples of magnetic fraction. Curve 1 — sample No. Bd-256/2 — glassy pyroxene-feldsparic andesite. The sample contains two magnetic phases — $T_{C1} \approx$ 480 °C; $T_{C2} \approx$ 590 °C. Curve 2 — sample No. Vt-45/11 — pyroxene andesite. The sample contains two magnetic phases $T_{C1} \approx$ 480 °C; $T_{C2} \approx$ 590 °C.

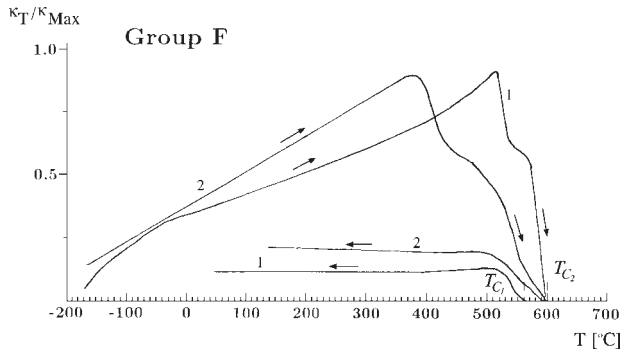

Fig. 7. Thermomagnetic curves of samples of magnetic fraction. Curve 1 — sample No. 329-B2 — pyroxene-hornblende andesite. The sample contains two magnetic phases — $T_{C1} \approx$ 530 °C; $T_{C2} \approx$ 590–600 °C. Sample No. KrVr-26/1 — hyperstene-augite andesite. The sample contains two magnetic phases — $T_{C1} \approx$ 420 °C; $T_{C2} \approx$ 600 °C.

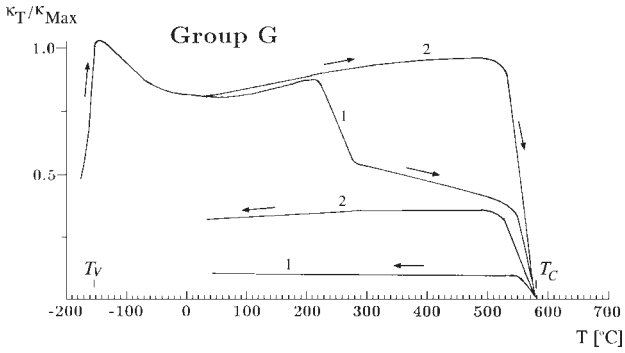

Fig. 8. Thermomagnetic curves of samples of magnetic fraction. Curve 1 — sample No. I-104/1 — propylized pyroxene andesite. The sample contains only one magnetic phase of $T_C \approx$ 580 °C and Verwey transition temperature $T_V \approx$ –153 °C. The sample showed very strong maghemitization in the interval 220–530 °C. Curve 2 — sample No. I-181/4-propylitized pyroxene andesite. The sample contains only one magnetic phase of $T_C \approx$ 580 °C and Verwey transition temperature $T_V \approx$ –153 °C.

We see from Tables 1–3, that quite frequently a presence of hematite in respective rocks has been interpreted on the basis of ore microscopy, Mössbauer spectroscopy and X-ray diffraction analysis. We know that pure stoichiometric hematite has pointed out very clear, reproducible Curie temperature of $T_C \approx$ 675 °C, Hopkinson's peak (Hp ≈ 650 °C) and the Morin transition temperature of about $T_M \approx$ –20 °C (Orlický 1994). No case of detection of Curie temperature of $T_C \approx$ 675 °C, Morin transition of $T_M \approx$ –20 °C or Hopkinson's peak of about 650 °C was found in these volcanic rocks. It means, no clear stoichiometric hematites occurred in the above mentioned rocks, but hematite-ilmenites should be present in these rocks. The presence of the hematite-ilmenites can be interpreted on the basis of their Curie (or Néel) temperatures, taking into account the theoretical linear dependence of T_C on the portion of ilmenite within hematite; $T_C \approx$ 675 °C corresponds to pure hematite and $T_C \approx$ –218 °C corresponds to pure ilmenite (Stacey & Banerjee 1974; McElhinny 1973; Nord & Lawson 1989). So, the compositional parameter $x \approx 0.09$–0.04 has been derived for Fe-Ti oxides of Curie temperatures within the range $T_C \approx$ 585–640 °C. This is supposed to be within the range of the hematite-rich components, which are as a consequence of slow cooling of titanohematites ($Fe_{2-x}Ti_xO_3$), according to the above mentioned statements.

We see from Tables 1–3 and in Figs. 3–10, that most of the rocks contain two magnetic phases, but some of them contain only one magnetic phase. The characteristic representative thermomagnetic curves of Fe-Ti oxides (Figs. 3–10) have been chosen on the basis of a comparison of the results of all the samples studied by this method (670 individual samples were studied; the T_C of the magnetic phase on each presented graph is inferred where the projected steepest part of the descending curve intersects the temperature axis; only the results during heating of the sample were considered for the detection of different magnetic phases on the basis Curie temperatures). We see from Figs. 3–7 and Fig. 9 that a relation between the magnetic phase of lower Curie temperature and that of higher T_C is different. In Figs. 8, 10, only one magnetic phase of Fe-Ti oxide was detected within the studied samples of rock.

Interpretation of the results

Seven dominant groups of magnetism carriers have been chosen on the basis of thermomagnetic curves and the relation of magnetic phases within the rocks. The mentioned groups have been designated B, C, D, F, G, I, and J (Tables 1–3 and in Figs. 3–10). The following characteristics of the individual groups are presented below.

Group B: the Fe-Ti oxides of the group contain two magnetic phases (Figs. 3, 4); a dominant phase ($T_{C1} \approx$ 130–220 °C) containing quasi homogeneous to partly oxidized TMs with a composition of $Fe_{2.35}Ti_{0.65}O_4$–$Fe2.5Ti_{0.5}O_4$, and the second- less abundant magnetic phase ($T_{C2} \approx$ 570 °C) which contains oxidized TMs.

Group C: Fe-Ti oxides contain two magnetic phases (Fig. 5): the first magnetic phase ($T_{C1} \approx$ 210 °C) corresponds to quasi homogeneous to partly oxidized TMs of composition $Fe_{2.5}Ti_{0.5}O_4$, and the second-phase $T_{C2} \approx$ 575 °C, which corresponds to oxidized TMs. The share of both phases is supposed to be equal in the rocks.

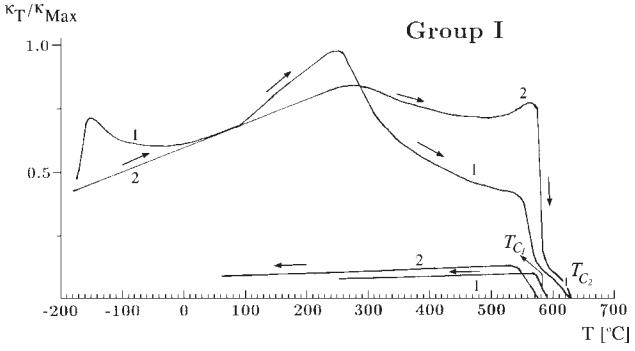

Fig. 9. Thermomagnetic curves of samples of magnetic fraction. Curve 1 — sample No. St-215/3; Curve 2 — sample No. St-156/1 — both samples are biotite-hornblende andesites. The samples contain two magnetic phases of $T_{C1} \approx 580$ °C and $T_{C2} \approx 620–630$ °C. The first phase of sample showed theVerwey transition temperature as well.

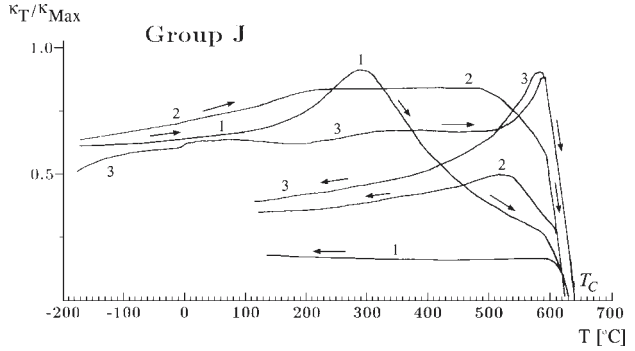

Fig. 10. Thermomagnetic curves of samples of magnetic fraction. Curve 1 — sample No. 3-IV-B1/1 — hornblende-pyroxene andesite. Curve 2 — sample No. St-201/4 — biotite-hornblende andesite. Curve 3 — sample No. St-TR-24/23 — hyperstene-hornblende-biotite andesite. All three samples contain only one magnetic phase of high Curie temperature-from $T_C \approx 620$ °C (curve 2) to $T_C \approx 640$ °C (curve 3). Sample 3-IV-B1/1 is highly maghemitized.

Group D: Fe-Ti oxides contain two magnetic phases (Fig. 6); the first — dominant magnetic phase of $T_{C1} \approx 480$ °C and the second magnetic phase of $T_{C2} \approx 590$ °C, which is in a minor portion in the sample. Both magnetic phases correspond to oxidized TMs of unknown composition. Hematite-ilmenites can be present in these minerals.

Group F: Fe-Ti oxides contain two magnetic phases (Fig. 7); the first magnetic phase of $T_{C1} \approx 420$ °C and $T_{C1} \approx 530$ °C, and the second magnetic phase of $T_{C2} \approx 600$ °C and $T_{C2} \approx 590–600$ °C. Both magnetic phases correspond to oxidized TMs with presence of hematite-ilmenites.

The magnetic minerals of groups B to F show a characteristic decreasing of κ from laboratory temperature down to liquid nitrogen temperature (Figs. 3–7). This behaviour reflects a presence of either quasi homogeneous or oxidized TMs.

Group G: The magnetic minerals of this group contain only one magnetic phase of $T_C \approx 580$ °C (and Verwey transition temperature of $T_V \approx -153$ °C (Fig. 8)). This magnetic phase corresponds to pure multi domain magnetite (a small portion of hematite-ilmenites can be present in these magnetic minerals).

Group I: The magnetic minerals of this group contain two magnetic phases, both of them with comparatively high Curie temperatures (Fig. 9; $T_{C1} \approx 580$ °C, $T_{C2} \approx 620–630$ °C). The first phase corresponds to magnetite (mostly non-stoichiometric), the second phase contains hematite-ilmenites.

Group J: The magnetic minerals contain only one magnetic phase of Curie temperatures in the range $T_C \approx 620–640$ °C. Hematite-ilmenites are present in the rocks of the group J. Ilmenites are frequently present in both I and J groups (see Tables 1–3). The composition of the hematite-ilmenites is supposed to be within the range of $x \approx 0.09–0.04$ for magnetic phases with Curie temperatures of $T_C \approx 585–640$ °C.

Magnetic minerals of the first phase of lower T_C of rocks of the D and F groups correspond to oxidized TMs, the second magnetic phase of higher T_C correspond probably also to oxidized TMs with a presence of hematite-ilmenites. According to McElhinny (1973) the composition of naturally occurring spinels tend to be displaced towards the ilmenite-hematite series in the direction of increased oxidation. So, we can predict that the hematite-ilmenites can also be present there in the rocks of the B, C, groups, despite not having been detected by applied methods. The compositions of oxidized TMs have not been derived due to lack of information about the degree of oxidation.

The occurrences of the above mentioned dominant groups of magnetism carriers have been delineated in the geological schemes (Figs.1, 2).

The Fe-Ti oxides of groups B and C (Figs. 3–5) have been revealed dominantly within the basalts and basaltic andesites (Figs.1, 2). Oxidized TMs of group D were revealed in pyroxene andesites, glassy pyroxene feldspharic andesites (Fig. 1) and olivine basalts, as well as in basaltic andesites (Figs.1, 2). Fe-Ti oxides of C and D groups were revealed mostly within the smaller individual lava flows, basaltic diatremes, volcanic cones, dykes and necks. Fe-Ti oxides of group F are frequently present in basaltic andesites, pyroxene andesites of the Kremnické vrchy Mts., in pyroxene and basaltic andesites as well as in hornblende and hyperstene hornblende andesites of the Poľana and Javorie Mts. (Fig. 1). Magnetites of group G were revealed mostly within the propylitized andesites and the most of intrusive rocks (Fig. 1; e.g. diorites, monzodiorites from borehole Kon-1, within the interval from ca. 1000 to 1800 m contain dominantly magnetite of the group G). The basalts of several localities contain minerals near to magnetite (Figs.1, 2). These types of Fe-Ti oxides were found mostly in basaltic bodies of different shapes (lava flows, volcanic cones and agglomerates together).

While the Fe-Ti oxides of the group I have been revealed very frequently in andesites of variable petrographic types, as well as in several localities of rhyolites, the Fe-Ti oxides of the group J occurred mostly within biotite-hornblende andesites, hornblende pyroxene andesite, hyperstene-hornblende andesites, as well as in most of rhyolites and rhyodacites (Fig. 1). TMs or oxidized TMs have never been found in rhyolites or rhyodacites.

Acknowledgements: I thank RNDr. J. Beňka, CSc., RNDr. A. Mihalíková who performed respectively the ore and transmission microscopy, RNDr. F. Caňo, who realized the elec-

tron microprobe analysis, Prof. Ing. J. Lipka, DrSc., and Ing. I. Tóth who performed the laboratory measurements and the interpretation of the Mössbauer spectroscopy, RNDr. B. Toman, who realized the laboratory measurements and the interpretation of the X-ray diffraction analysis, and Doc. RNDr. A. Zentko, DrSc., who studied the change of electric voltage of samples influenced by temperature in the interval from laboratory temperature down to liquid helium temperature. Many thanks Doc.RNDr.I.Rojkovič,DrSc., and RNDr.J.Lexa,CSc., for stimulating discussions and very appreciable improvement of early version of the manuscript.

References

Ade Hall J.M., Palmer H.C. & Hubbard T.P., 1971: The magnetic and petrological response of basalts to regional hydrothermal alteration. *Geophys. J. Roy. Astron. Soc.,* 24, 137–17.

Banerjee S.K. & O'Reilly W., 1967: Mössbauer-effect measurements in Fe-Ti spinels with local disorder. *J. of Apl. Phys.,* 38, 3, 1289–1290.

Ehlers E.G. & Blatt H., 1980: Petrology, Igneous, Sedimentary and Metamorphic. *W.H. Freeman and Company,* San Francisco.

Furuta T., 1993: Magnetic properties and ferromagnetic mineralogy of oceanic basalts. *Geophys. J. Int*., 113, 95–114.

Hamano Y., 1989: Lattice constants of titanomagnetites at high temperatures. *J. Geomag. Geoelectr*., 41, 65–75.

Hargraves R.B. & Petersen N., 1971: Notes on the correlation between petrology and magnetic properties of basaltic rocks. *Z. Geophys.,* 37, 367–382.

Konečný V., Lexa J. & Planderová E., 1983: Stratigraphy of the Central Volcanic Fields. *Západ. Karpaty, Sér. Geol.,* 9 (in Slovak).

Kropáček V., Lašťovičková M. & Bochníček J., 1981: Magnetic and electrical properties of basaltic rocks from South-Eastern Slovakia. *Sbor. Geol. Věd, ř. UG*, 17, 87–100.

Kropáček V., 1985: Magnetic properties of young alkaline volcanic rocks of Central Europe. *(Doctorant's Thesis). Manuscript; The Geophysical Institute of the Czechoslovak Republic*, Prague, (in Czech).

Lexa J., Konečný V., Kaličiak M., Hojstričová V., 1993: A space-time distribution of volcanics in the Carpatho-Pannonian region. Geodynamic model and deep-seated pattern of the West Carpathians. *GÚDŠ,* Bratislava, 57–69 (in Slovak).

Lexa J., Konečný P., Hojstričová V., Konečný V. & Köhlerová M., 1997: The petrographical model of the Štiavnica Mts.´s Stratovolcano. *Manuscript. In the Archives of the Geological Survey of Slovak Republic,* Bratislava (in Slovak).

Lawson Ch.A., Nord Jr.G.L. & Champion D.E., 1987: Fe-Ti oxide mineralogy and the origin of normal and reverse remanent magnetization in dacite pumice blocks from Mt. Shasta, California. *Phys. Earth Planet. Inter.,* 46, 270–288.

Lipka J., Hucl M., Prejsa M., Tóth I., Cirák J., Gábriš F., Sitek J., Grone R., Červeň I., Seberíni M., Metko E., Štubendek M., 1982-1988: Mössbauer spectroscopy of natural minerals. *(I–VI stage, Manuscripts). The laboratory of the Nuclear Physic Dept. of the Slovak Technical University,* Bratislava (in Slovak).

McElhinny M.W., 1973: Palaeomagnetism and plate tectonics. *Cambridge University Press,* 1–357.

Mihalíková A. & Šímová M., 1989: The geochemistry and petrology of the Miocene-Pleistocene alkaline basalts of central and southern Slovakia. *Západ. Karpaty, Ser. Miner., Geochem., Metallogen.,* 12, 7–142 (in Slovak).

Moskowitz B.M., 1987: Towards resolving the inconsistencies in characteristic physical properties of synthetic titanomaghemites. *Phys. Earth Planet. Inter*., 46, 173–183.

Nord Jr. G.L. & Lawson Ch.A., 1989: Order-disorder transition-induced twin domains and magnetic properties in ilmenite-hematite. *Amer. Mineralogist,* 74, 160–176.

O'Donovan J.B. & O'Reilly W., 1977: The preparation, characterization and magnetic properties of sythetic analogues of some carriers of the palaeomagnetic record. *Adv. Earth Planet. Sci.,* 1, 99–112.

O'Reilly W., 1984: Rock and mineral magnetism. *Blackie,* Glasgow, 1–222.

Orlický O., Kropáček V. & Vass D., 1982: Palaeomagnetism and radiometric ages of alkaline basalts of SW Slovakia. *Miner. slovaca*, 14, 97–116 (in Slovak).

Orlický O., 1990: Detection of magnetic carriers in rocks: results of susceptibility changes in powdered rock samples induced by temperature. *Phys. Earth. Planet. Inter*., 63, 66–70.

Orlický O., 1992: Paleomagnetism—Štiavnické, vrchy and Pohronský Inovec Mts., Vtáčnik Mts., Kremnické vrchy Mts., Javorie and Poľana Mts. *(Manuscript). Geophysical Institute of the Slovak Academy of Sciences,* Bratislava (in Slovak).

Orlický O., Caňo F., Lipka J., Mihaliková A. & Toman B., 1992: Fe-Ti magnetic minerals of basaltic rocks: A study of their nature and composition. *Geol. Carpathica*, 43, 5, 287–293.

Orlický O., 1993: Palaeomagnetism and magnetic mineralogy of selected neovolcanic rocks of the Central Slovakia. *Geol. Carpathica*, 44, 6, 399–408.

Orlický O., 1994: Study and detection of magnetic minerals by means of the measurements of their low-field susceptibility changes induced by temperature. *Geol. Carpathica*, 45, 113–119.

Orlický O., 1996: Curie temperatures of the Fe-Ti oxides of basalts: Is it possible to use Curie temperatures to assess the source of the depth of origin of the Fe-Ti oxides and related basalt magmas? *Geol. Carpathica*, 47, 1, 51–58.

Orlický O., Balogh K., Konečný V., Lexa J., Túnyi I. & Vass D., 1996: Paleomagnetism and radiometric ages of basalts of Central and Southern Slovakia (Western Carpathians). *Geol. Carpathica*, 47,1, 21–30.

Pašteka V., 1991: Identification of Magnetic Minerals at Low Temperatures. *Acta Geol. Geogr. Univ. Comen., Geol.,* 47/II, 121–125.

Radhakrishnamurty C., Likhite S.D., Deutsh E.R. & Murthy G.S., 1981: A comparison of the magnetic properties of synthetic titanomagnetites and basalts. *Phys. Earth Planet. Inter.,* 26, 37–46.

Radhakrishnamurty C. & Likhite S.D., 1993: Frequency dependence of low-temperature susceptibility peak in some titanomagnetites. *Phys. Earth Planet. Inter*., 76, 131–135.

Readman P.W. & O'Reilly W., 1970: The synthesis and inversion of non-stoichiometric titanomagnetites. *Phys. Earth Planet. Inter*., 4, 121–128.

Stacey F.D. & Banerjee S.K., 1974: The physical principles of rock magnetism. *Elsevier*, Amsterdam, 1–195.

Syono Y. & Ishikawa Y., 1963: Magnetocrystalline anisotropy of $xFe_2TiO4(1-x)Fe_3O4$. *J. Phys. Soc. Jpn*., 18; 1230–1231.

Senanayake W.E. & McElhinny M.W., 1982: The effects of heating on low-temperature susceptibility and hysteresis properties of basalts. *Phys. Earth Planet. Inter.,* 30, 317–321.

Warner B.N., Shive P.N., Allen J.L. & Terry C., 1972: A Study of the hematite-ilmenite series by the Mössbauer Effect. *J. Geomag. Geoelectr*., 24, 353–367.